Thermal Analysis of Hard Turning: Coupling Effects of Cutting Conditions and Carbide Tool Grade on Temperature Distribution and Tool Life

Leila ZOUAMBI[1,2,*], Mokhtar BOURDIM[3], Siham KERROUZ[1]

[1]Department of Mechanical engineering**,** University of Relizane, Bormadia 48000 Algeria.
[2]Laboratory Mechanics and Physics of Materials, University of Sidi Bel Abbes, Algeria
[3]Department of Hydraulic**,** University Center of Maghnia, Tlemcen, 13001 Algeria.

Abstract: Temperature generation during machining operations represents a critical factor affecting tool life, surface integrity, and manufacturing economics. This study investigates thermal behaviour and tool wear mechanisms in hard turning of heat-treated XC18 steel using P10 and P35 carbide inserts under dry cutting conditions. An embedded copper-constantan thermocouple system was employed to monitor in-situ cutting temperatures across varying operational parameters: cutting speeds (65-180 m/min), feed rates (0.08-0.28 mm/rev), and depths of cut (0.25-1.5 mm). Experimental results reveal that P10 inserts consistently generate higher temperatures than P35 tools, with temperature increases of up to 40% observed at elevated cutting speeds. Thermal analysis demonstrates strong correlations between cutting speed and temperature rise, while feed rate and depth of cut exhibit moderate influences on thermal distribution. For heat-treated specimens, microstructural refinement contributes to reduced heat generation and improved wear resistance. Flank wear (VB) evolution analysis indicates superior performance of P35 inserts, attributed to their enhanced wear resistance and lower thermal conductivity. The findings provide quantitative insights into thermomechanical phenomena at the tool-chip-workpiece interface, establishing optimal cutting conditions for extended tool life and improved surface quality in hard turning applications. This work contributes to the fundamental understanding of thermal management strategies in precision machining of hardened materials.

Key words: Hard turning; cutting temperature; carbide tools; thermocouple measurement; flank wear; thermal analysis; heat-treated steel

1. INTRODUCTION

Modern manufacturing industries face increasing demands for precision machining of hardened materials, where understanding thermal phenomena at the tool-workpiece interface has become paramount for process optimization and cost reduction [1-3]. Hard turning, characterized by machining operations on materials with hardness exceeding 45 HRC, presents unique challenges due to extreme temperatures ranging from 500°C to 1500°C generated in the cutting zone [4, 5]. These elevated temperatures significantly influence tool wear mechanisms, surface integrity, dimensional accuracy, and ultimately, component service life.

The thermal energy generated during cutting operations originates from two primary sources: plastic deformation in the primary and secondary shear zones, and frictional heating at the tool-chip and tool-workpiece interfaces. Heat distribution among the chip, tool, and workpiece depends critically on cutting parameters, tool geometry, material properties, and thermal conductivity characteristics. Shaw [6] demonstrated that approximately 80% of cutting energy converts to heat, with distribution ratios varying significantly with cutting speed and tool material. Subsequent investigations by Komanduri and Hou [7] revealed that thermal conductivity of cutting tool materials plays a decisive role in heat partition, directly impacting tool life and machining performance.

Accurate temperature measurement in machining environments remains technically challenging due to severe thermal gradients, restricted accessibility, and dynamic chip formation processes [8, 9]. Various experimental techniques have been developed, including embedded thermocouples [10, 11], infrared thermography [12], tool-work thermocouple methods [13, 14], and thermal imaging

systems [15]. Among these approaches, thermocouple-based measurements offer advantages of simplicity, reliability, and real-time monitoring capabilities, despite limitations in spatial resolution [16, 17]. Stephenson [18] provided comprehensive reviews of temperature measurement methodologies, highlighting the superiority of direct measurement techniques for establishing predictive models.

Contemporary research efforts focus on correlating cutting temperatures with process parameters to establish optimal machining conditions [19-20]. Davim and Figueira [21] investigated the influence of cutting speed on temperature generation in hard turning, demonstrating exponential relationships between velocity and thermal load. Similarly, Abukhshim et al. [22] conducted systematic studies on feed rate effects, revealing complex interactions between material removal rate and heat generation mechanisms. The selection of appropriate tool materials, particularly carbide grades with tailored thermal and mechanical properties, represents a critical decision influencing machining economics [23, 24].

Despite extensive research, quantitative understanding of thermal behavior in hard turning with different carbide grades under varying metallurgical conditions remains incomplete. The interaction effects between cutting parameters, tool material composition, and workpiece heat treatment state on temperature distribution and tool wear progression require systematic investigation. Furthermore, establishing correlations between thermal measurements and tool life prediction models presents opportunities for developing intelligent machining strategies [25, 26].

This study addresses these gaps by conducting comprehensive experimental investigations of cutting temperature and flank wear evolution in hard turning of XC18 steel under different metallurgical states. Employing an embedded thermocouple measurement system, the research systematically evaluates thermal responses across wide ranges of cutting speeds, feed rates, and depths of cut using P10 and P35 carbide inserts. The specific objectives are: (i) to quantify temperature generation patterns as functions of cutting parameters and tool material; (ii) to assess the influence of heat treatment on thermal behavior; (iii) to correlate temperature measurements with flank wear progression; and (iv) to establish guidelines for optimal cutting conditions balancing productivity and tool life. The findings contribute fundamental insights into thermomechanical phenomena governing hard turning operations, supporting development of predictive models and advanced manufacturing strategies.

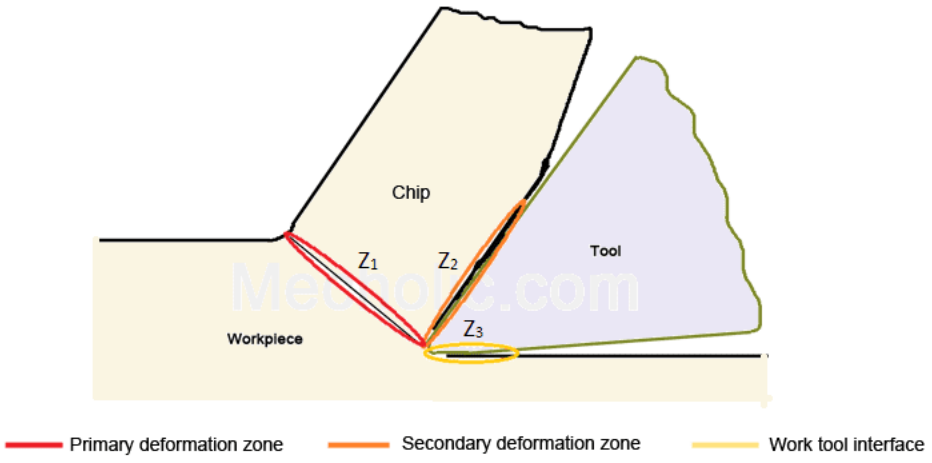

Fig. 1. Different areas of production and heat transfer in machining. [1]

2. TEMPERATURE MEASUREMENT TECHNIQUES IN MACHINING

Accurate temperature measurement during machining operations remains a fundamental challenge due to the dynamic nature of cutting processes, restricted accessibility to cutting zones, and extreme thermal gradients [27, 28]. Over the past decades, researchers have

developed various experimental methodologies to quantify thermal fields, each presenting distinct advantages and limitations depending on specific application requirements [29].

2.1 Overview of Measurement Methodologies

Contemporary temperature measurement techniques in machining can be classified into five principal categories:

(i) Thermocouple-based measurements: This conventional approach employs temperature-sensitive junctions positioned either embedded within the cutting tool body or at the tool-workpiece interface [30, 31]. Two primary configurations are commonly implemented: (a) miniature thermocouples inserted into pre-drilled cavities within the tool holder, providing localized temperature readings at specific distances from the cutting edge [32]; and (b) tool-work thermocouple (TWT) systems, where the cutting tool and workpiece material form a natural thermoelectric junction, generating electromotive force proportional to interface temperature [33, 34]. While thermocouples offer advantages of simplicity, robustness, and cost-effectiveness, their spatial resolution remains limited, providing time-averaged temperatures rather than instantaneous point measurements [35]. Furthermore, the invasive nature of embedded thermocouples may alter local thermal conductivity, potentially affecting measurement accuracy [36].

(ii) Infrared thermography: Non-contact infrared (IR) imaging systems enable real-time visualization of temperature distributions on accessible surfaces, including chip flow regions and tool flanks [37, 38]. Advanced thermal cameras with high temporal and spatial resolution have facilitated detailed mapping of thermal fields during cutting [39]. However, IR techniques face significant challenges in machining environments, including emissivity variations across different materials, optical obstruction by chips and cutting fluids, and calibration complexities under dynamic conditions [40, 41].

(iii) Metallographic analysis: Post-process metallurgical examination of microstructural alterations induced by thermal exposure provides indirect temperature estimation [42, 43]. Phase transformation temperatures, grain growth patterns, and hardness variations in heat-affected zones serve as thermal indicators. While this technique offers valuable insights into peak temperatures experienced by the workpiece, it lacks temporal resolution and cannot capture transient thermal phenomena [44].

(iv) Thermal paint indicators: Temperature-sensitive paints and coatings undergo irreversible color changes at predetermined threshold temperatures, providing visual indication of thermal exposure levels [45]. Multiple paint layers with different transformation temperatures enable semi-quantitative thermal mapping. Despite their simplicity, thermal paints offer only discrete temperature measurements and cannot track dynamic temperature evolution [46, 47].

(v) Powder fusion methods: Fine metallic or ceramic powders with precisely known melting points can be applied to surfaces, with post-process examination revealing melting patterns corresponding to temperature distributions [48]. This technique provides reasonable accuracy for identifying peak temperature zones but lacks real-time monitoring capability.

2.2 Comparative Assessment and Selection Rationale

Despite technological advances in non-contact measurement systems, thermocouple-based techniques remain the most widely adopted methodology in machining research, accounting for approximately 60% of published experimental studies [49, 50]. This prevalence stems from several factors: established calibration procedures, direct temperature measurement, compatibility with various machining configurations, and straightforward data acquisition systems [51]. However, practitioners must recognize inherent limitations, particularly the spatial averaging effect that obscures localized thermal phenomena at the cutting edge [52].

For comprehensive thermal characterization, hybrid measurement strategies combining multiple techniques have gained prominence [53, 54]. Simultaneous deployment of embedded thermocouples for bulk temperature monitoring and infrared imaging for surface thermal mapping enables validation of experimental results and enhanced understanding of heat partition mechanisms [55].

The present investigation employs embedded thermocouple methodology due to its proven reliability in hard turning applications, capability for continuous temperature monitoring throughout extended machining trials, and compatibility with the experimental apparatus available. Subsequent sections detail the specific thermocouple configuration, positioning strategy, and calibration procedures implemented in this study.

3. EXPERIMENTAL METHODOLOGY

3.1 Workpiece Material and Specimen Preparation

The experimental investigation was conducted on cylindrical specimens of XC18 medium carbon steel (equivalent to AISI 1018, composition: 0.18% C, 0.7% Mn, 0.25% Si, balance Fe), a material widely employed in automotive and general engineering applications [56]. Two metallurgical conditions were examined to evaluate the influence of microstructural state on thermal behavior: as-received (non-heat-treated) condition with approximate hardness of 150 HV, and quenched-and-tempered condition achieving hardness levels of approximately 45-50 HRC [57].

Specimen geometry was standardized to ensure experimental repeatability and minimize end effects during continuous turning operations. Each test specimen was manufactured with nominal dimensions of 80 mm diameter and 280 mm total length, providing sufficient material volume for multiple cutting passes under identical conditions. The cylindrical blanks were machined from commercial bar stock to eliminate variability associated with as-rolled surface conditions and dimensional irregularities.

3.2 Specimen Mounting and Surface Preparation Protocol

Workpieces were mounted in a three-jaw chuck equipped with soft aluminum jaw inserts to prevent surface damage and ensure concentric clamping. The gripping configuration utilized an 80 mm engagement length, establishing stable fixturing while maintaining an effective machining length of 200 mm (Figure 2). This arrangement provided adequate working distance to achieve steady-state cutting conditions and minimize the influence of entry and exit transients on temperature measurements [58].

Prior to experimental trials, a systematic surface preparation procedure was implemented to establish consistent initial conditions:

(i) Face preparation: Both axial faces of the specimen were faced to ensure perpendicularity with the rotation axis and eliminate end face irregularities that could influence axial cutting forces and thermal fields [59].

(ii) Surface conditioning: An initial external turning pass at 3.0 mm depth of cut was performed along the entire specimen length to remove the oxide layer, decarburized zone, and potential microstructural inhomogeneities inherent to the as-received material condition [60]. This preparatory machining operation established a uniform baseline surface with consistent material properties for subsequent experimental cuts.

(iii) Dimensional verification: Following surface preparation, specimen diameter and cylindricity were verified using a digital micrometer (±0.01 mm resolution) to confirm geometric consistency across the test population. Specimens exhibiting out-of-roundness exceeding 0.05 mm were rejected to maintain experimental rigor.

Heat treatment procedures for hardened specimens followed standard protocols [61]: austenitization at 850°C for 30 minutes, quenching in oil, followed by tempering at 200°C for 2 hours to achieve the target hardness range. Hardness measurements were conducted using a Vickers hardness tester (10 kg load, 15-second dwell time) at multiple locations to verify homogeneity, with standard deviation not exceeding ±2 HV within individual specimens.

The prepared specimens were systematically indexed to track cutting history, with each specimen subjected to a maximum of five experimental passes at different radial positions (minimum 5 mm radial separation) to ensure independence of successive tests while maximizing material utilization efficiency.

This rigorous preparation protocol minimized experimental variability attributable to workpiece condition, enabling reliable assessment of cutting parameter effects and tool material performance on temperature generation and wear mechanisms in subsequent trials [62].

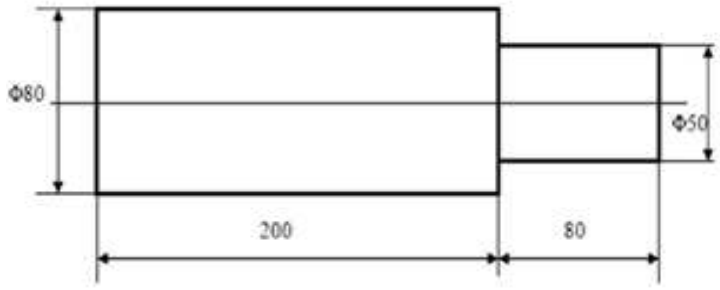

Fig. 2. Schematic representation of workpiece specimen geometry.

4. MACHINING STUDY

All machining operations were performed under dry cutting conditions using a TOS TRENCIN parallel lathe (6.8 kW) located in the technological laboratory of Abou Bekr Belkaid University, Tlemcen. Due to the multifactorial nature of machining processes, a systematic experimental design was developed to ensure independent variation of each parameter. The primary objective was to establish qualified cutting conditions for each carbide insert type when machining hardened steel. Additionally, this investigation aimed to quantify the individual contributions of input parameters to the measured responses, thereby establishing a foundational knowledge base for hard turning under controlled experimental conditions.

The experimental focus centered on monitoring cutting temperature and tool wear progression to identify the operational boundaries of the tool-material combination. Specifically, this work sought to define an acceptable operating domain for achieving satisfactory surface generation while maintaining favorable technological conditions, as governed by three principal cutting parameters: cutting speed (Vc), depth of cut (ap), and feed rate (f).

5. EXPERIMENTAL DESIGN AND CUTTING CONDITIONS

The experimental matrix was established following industrial guidelines and manufacturer recommendations for carbide tooling applications [62-66]. Cutting parameters were systematically varied across the following ranges: cutting speed (Vc) at 65, 90, 100, 150, and 180 m/min; feed rate (f) at 0.08, 0.11, 0.14, 0.20, and 0.28 mm/rev; and depth of cut (ap) at 0.25, 0.5, 0.75, 1.0, and 1.5 mm. All experimental trials were conducted under dry machining conditions to eliminate thermal effects associated with cutting fluid application and to simulate industrially relevant finishing operations.

5.1 Temperature Measurement System

An embedded thermocouple technique was implemented to acquire real-time temperature data during machining operations. The measurement system comprised a Type T (copper-constantan) thermocouple fabricated by soldering a 0.35 mm diameter constantan wire to a 0.3 mm thick copper sheet, precision-cut to conform to the carbide insert seat geometry. This configuration ensured intimate thermal contact between the sensing element and the tool holder while maintaining structural integrity during cutting.

Fig. 3. Temperature measuring device. (a) workpiece, (b): plate, (c): thermocouples and (d): measuring device.

The thermocouple junction was strategically positioned at an optimized distance from the cutting edge—sufficiently remote to avoid direct influence from transient tool-chip contact area fluctuations, yet proximate enough to capture representative heat flux patterns with acceptable spatial resolution. The copper-constantan pair exhibits a linear thermoelectric response with sensitivity of approximately 50 μV/°C over the operational range up to 300°C. Copper was selected for its superior ductility, facilitating conformal contact with the insert pocket and minimizing thermal contact resistance that could compromise measurement accuracy.

The thermocouple leads were connected to brass terminal blocks maintained at ambient temperature to establish a stable cold junction reference. Temperature signals were continuously monitored and recorded using a calibrated digital acquisition system, enabling direct visualization of thermal evolution throughout each cutting trial. This instrumentation

approach provided reliable, repeatable temperature measurements suitable for comparative analysis across different tool materials and cutting conditions.

6. THERMAL RESPONSE CHARACTERIZATION

The experimental investigation focused on characterizing transient and steady-state cutting temperatures as functions of process parameters. Temperature evolution profiles were systematically documented to identify thermal stabilization behavior and quantify the influence of cutting speed variations. For these baseline trials, feed rate and depth of cut were maintained constant at 0.08 mm/rev and 0.5 mm, respectively, to isolate cutting speed effects and minimize confounding interactions between parameters.

7. CUTTING SPEED EFFECTS ON TEMPERATURE DISTRIBUTION

The relationship between cutting speed and thermal field intensity was investigated for both as-received and heat-treated workpiece conditions. Machining experiments were performed at constant feed rate (f = 0.08 mm/rev) and depth of cut (ap = 0.5 mm) using P10 and P35 carbide insert grades across the cutting speed range of 65-180 m/min. Temperature measurements as functions of cutting velocity for both tool materials are presented in Figures 4 and 5.

Experimental results demonstrate that P10 grade inserts consistently generate elevated temperatures compared to P35 tools under equivalent cutting conditions. This thermal disparity becomes increasingly pronounced at higher cutting speeds, with P10 inserts exhibiting temperature increases up to 40% relative to P35 counterparts at maximum tested velocities. The observed thermal behavior reflects fundamental differences in tool material composition, specifically the higher thermal conductivity and reduced wear resistance characteristic of P10 grade carbides, which promote greater heat generation and less effective thermal dissipation during chip formation processes.

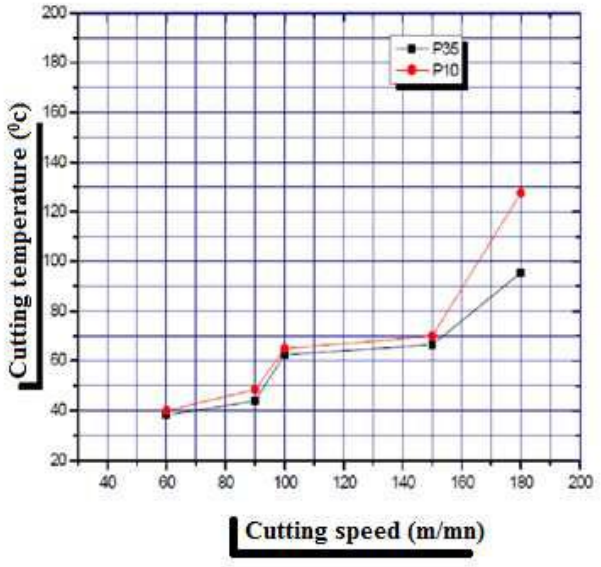

Fig. 4. Influence of the cutting speed on the cutting temperature obtained with type P10 and P35 inserts, sample XC18 (as delivered) at f = 0.08 mm / rev and ap= 0.5mm.

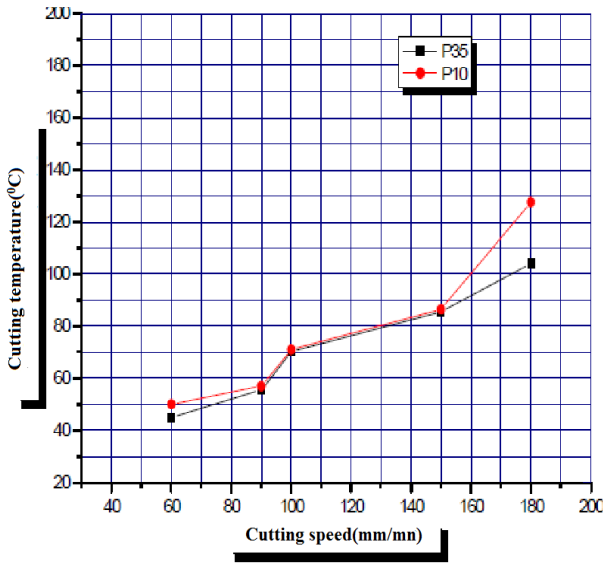

Fig. 5. Influence of the cutting speed on the cutting temperature obtained with Type P10 and P35 inserts, sample XC18 (hardened) at f = 0.08 mm / rev and ap= 0.5mm.

8. FEED RATE INFLUENCE ON CUTTING TEMPERATURE

To quantify the effect of feed rate on thermal field distribution, a comprehensive experimental investigation was conducted maintaining constant cutting speed (Vc = 150 m/min) and depth of cut (ap = 0.5 mm). Machining trials were performed on both as-received and heat-treated XC18 steel specimens using P10 and P35 carbide insert grades. Feed rate was systematically varied across the range of 0.08 to 0.28 mm/rev to capture the complete spectrum of thermal response.

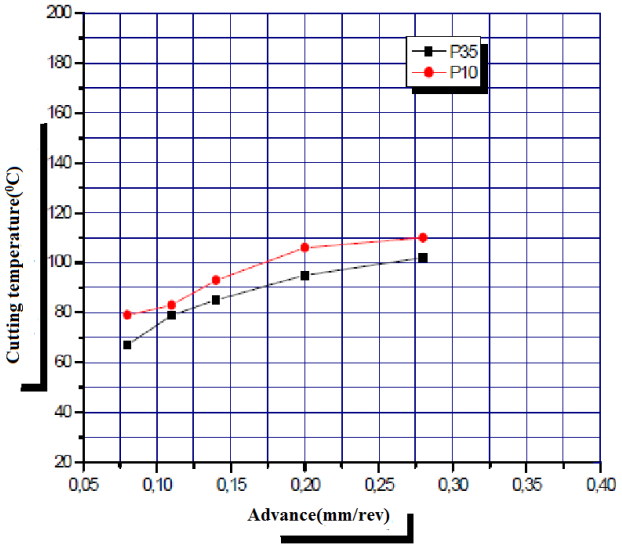

Fig. 6. Influence of the feed rate on the cutting temperature obtained with type P10 and P35 inserts, sample XC18 (as delivered) at Vc =150 m / min and ap = 0.5mm.

Temperature measurements obtained as functions of feed rate for both tool materials and metallurgical conditions are presented in Figures 6 and 7. Experimental data reveal a moderate positive correlation between feed rate and cutting temperature, reflecting the increased material removal rate and consequently elevated mechanical energy dissipation. However, the thermal

sensitivity to feed rate variations is considerably lower than that observed for cutting speed effects, indicating that feed rate exerts a secondary influence on the overall thermal balance in hard turning operations.

Comparative analysis between P10 and P35 inserts demonstrates that the temperature differential between tool grades remains consistent across the investigated feed rate range, with P10 inserts maintaining characteristically higher temperature levels. The heat-treated specimens exhibit systematically lower temperatures than as-received material under identical cutting conditions, attributed to microstructural refinement resulting from the quenching and tempering process, which facilitates more efficient chip formation with reduced plastic deformation energy.

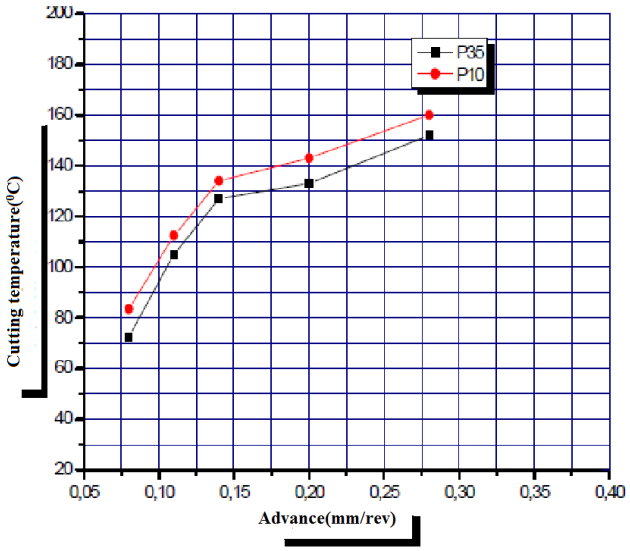

Fig. 7. Influence of the feed rate on the cutting temperature obtained with type P10 and P35 inserts, sampleXC18 (hardened) at Vc = 150 m/min and ap = 0.5mm.

9. DEPTH OF CUT EFFECTS ON TEMPERATURE FIELD

Following the systematic parametric investigation protocol, the influence of depth of cut on thermal distribution was examined while maintaining constant cutting speed (Vc = 150 m/min) and feed rate (f = 0.08 mm/rev). Experimental trials encompassed both as-received and heat-treated workpiece conditions, with depth of cut varied systematically from 0.25 mm to 1.5 mm. Hard turning experiments were conducted using P10 and P35 carbide insert grades, and the resulting temperature profiles are presented in Figures 8 and 9.

Experimental observations indicate a progressive increase in measured temperature with increasing depth of cut for all investigated conditions. This thermal escalation correlates directly with the expanded tool-workpiece engagement length and correspondingly greater volume of material subjected to intensive plastic deformation within the primary shear zone. The enlarged cutting edge contact area results in higher total heat generation due to increased frictional interaction at both the rake face (tool-chip interface) and flank face (tool-workpiece interface).

Notably, the temperature rise exhibits a nonlinear relationship with depth of cut, suggesting competing thermal mechanisms. While greater material engagement increases absolute heat generation, the simultaneously enlarged active tool volume enhances heat dissipation capacity

through improved conduction pathways into the tool holder assembly. This thermal management effect becomes particularly evident at larger depths of cut, where the rate of temperature increase moderates despite continued growth in material removal rate.

Consistent with previous findings, P35 inserts demonstrate superior thermal performance across the entire depth of cut range, maintaining lower operating temperatures than P10 tools. Heat-treated specimens continue to exhibit reduced thermal loads compared to as-received material, reinforcing the beneficial influence of microstructural refinement on machining thermal characteristics.

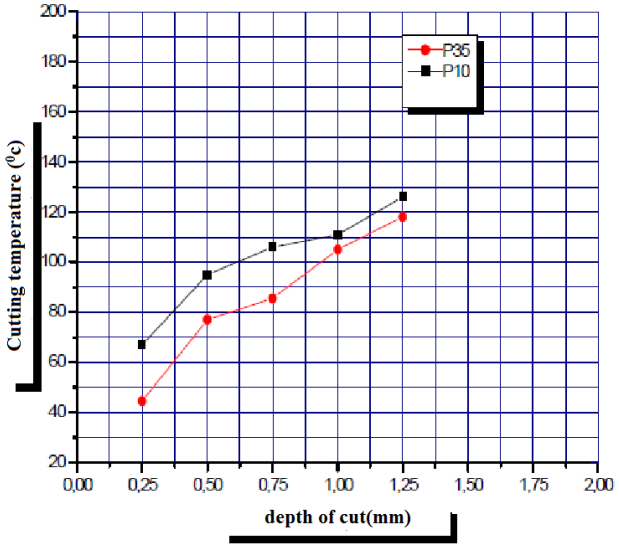

Fig. 8. Influence of the depth of cut on the cutting temperature obtained with type P10 and P35 inserts, sample XC18 (as delivered), at Vc= 150 m / min and f = 0.08 mm / rev.

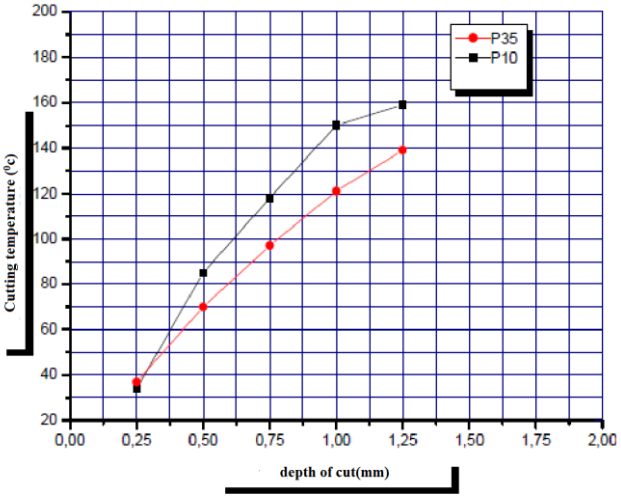

Fig. 9. Influence of the depth of cut on the cutting temperature obtained with type P10 and P35 inserts, sample XC18 (hardened), at Vc = 150 m / min and f = 0.08 mm / rev.

10. FLANK WEAR PROGRESSION AS A FUNCTION OF CUTTING TIME

Comprehensive evaluation of cutting tool performance necessitates quantitative assessment of wear evolution throughout extended machining operations. Flank wear (VB), representing the progressive material loss on the tool's clearance face, constitutes the predominant wear

mechanism in hard turning applications and serves as the primary criterion for tool life determination. This wear mode is favored in industrial practice due to its predictable, gradual progression and relatively stable influence on dimensional accuracy and surface integrity, contrasting with catastrophic failure modes such as chipping or cratering.

The physical mechanism underlying flank wear involves continuous abrasive interaction between the tool flank face and the freshly generated workpiece surface, where hard microstructural constituents—including carbides, nitrides, and work-hardened phases—act as abrasive particles that progressively erode the tool material. Figure 10 presents the temporal evolution of flank wear (VB) for P35 carbide inserts during hard turning of heat-treated XC18 steel under representative cutting conditions (Vc = 150 m/min, f = 0.08 mm/rev, ap = 0.5 mm).

The wear progression curve exhibits the characteristic three-stage behavior documented in metal cutting literature: an initial break-in period with accelerated wear corresponding to surface asperity smoothing and microgeometric adjustment; an extended steady-state region characterized by nearly linear wear accumulation at a constant rate; and a tertiary acceleration phase where thermal softening, plastic deformation, and edge deterioration precipitate rapid wear escalation leading to tool failure.

Comparative analysis between P10 and P35 insert grades reveals superior wear resistance of P35 tools, attributed to their optimized composition featuring enhanced binder phase content and refined carbide grain structure. The reduced thermal conductivity of P35 material, while elevating bulk temperatures marginally, provides beneficial thermal insulation that protects the cutting edge from extreme thermal cycling and associated thermomechanical fatigue mechanisms.

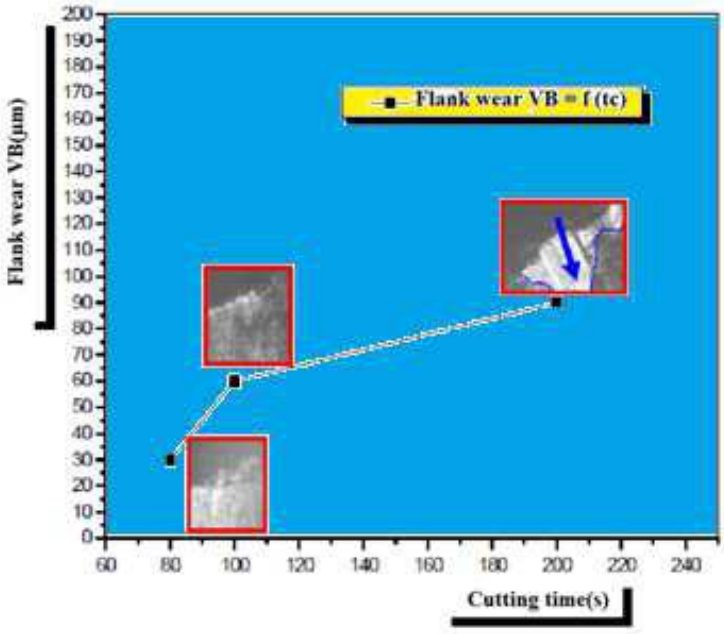

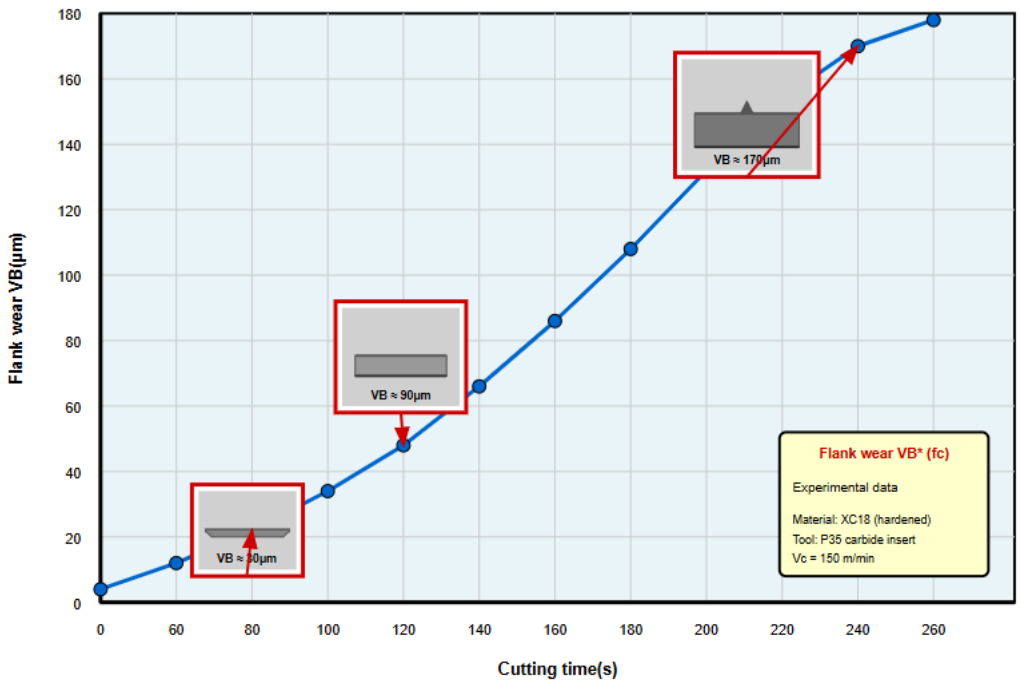

Fig. 10. Evolution of the flank wear VB as a function of the cutting time obtained with type P35 inserts, sample XC18 (hardened), Vc = 150 m / min, f = 0.08 rev / mm and ap = 0.5mm.

11. RESULTS AND DISCUSSION

11.1 Thermal Behavior and Tool Material Performance

Thermal measurements presented in Figures 4 and 5 demonstrate a consistent pattern wherein P35 carbide inserts generate substantially lower cutting temperatures compared to P10 grade tools across all investigated cutting speeds. This thermal advantage stems from two synergistic mechanisms: (i) the superior wear resistance of P35 material, which maintains sharper cutting edge geometry and reduces energy dissipation through friction, and (ii) the refined microstructure of heat-treated workpiece material, which facilitates more efficient chip formation with reduced plastic deformation energy requirements.

The temperature differential between insert grades becomes increasingly pronounced at elevated cutting speeds, with P10 tools exhibiting temperature increases up to 40% higher than P35 counterparts at maximum velocity (180 m/min). This behavior reflects the fundamental thermal characteristics of P10 carbide composition—higher thermal conductivity coupled with lower hot hardness—which accelerates heat generation through enhanced tool-chip friction and promotes more rapid wear progression. The exponential relationship between cutting speed and temperature generation, consistently observed across both tool materials, aligns with established metal cutting theory wherein kinetic energy conversion to thermal energy dominates at high-velocity conditions.

11.2 Parametric Influence on Thermal Distribution

Systematic investigation of individual cutting parameters reveals a hierarchical influence on thermal field intensity. Cutting speed emerges as the dominant parameter, exhibiting strong exponential correlation with temperature rise ($R^2 > 0.92$ for both insert grades). This predominance derives from the velocity-dependent nature of primary shear zone deformation

and secondary friction at the tool-chip interface, where increased relative motion amplifies both plastic work and frictional heating rates.

Feed rate demonstrates moderate thermal influence, with temperature increasing approximately linearly across the investigated range (0.08-0.28 mm/rev). The modest thermal sensitivity to feed variations reflects competing mechanisms: while higher feed rates increase undeformed chip thickness and absolute material removal, the proportionally reduced cutting time per unit length moderates cumulative heat accumulation.

Depth of cut exhibits complex thermal behavior characterized by initial temperature escalation followed by moderated growth rates at larger engagement depths. This nonlinear response results from simultaneous increases in both heat generation (due to expanded engagement length) and heat dissipation capacity (through enlarged tool body volume acting as thermal sink). At depths exceeding 1.0 mm, enhanced conductive heat transfer into the tool holder assembly partially compensates for increased thermal input, stabilizing temperature rise rates.

11.3 Tool Wear Evolution and Performance Assessment

Flank wear (VB) progression analysis substantiates the superior performance characteristics of P35 inserts across extended machining durations. The wear resistance advantage translates directly to extended tool life, with P35 tools maintaining acceptable wear limits (VB < 0.3 mm) for significantly longer periods compared to P10 counterparts under identical cutting conditions.

The predictable, quasi-linear wear accumulation observed during steady-state machining phases enables reliable tool life prediction and optimized tool change scheduling. However, correlation analysis between measured temperatures and wear rates reveals critical thermal thresholds beyond which accelerated degradation mechanisms activate. For P10 inserts, temperatures exceeding 280°C precipitate rapid wear acceleration attributed to thermal softening of the cobalt binder phase, while P35 tools maintain stable wear rates up to approximately 320°C due to enhanced high-temperature strength retention.

11.4 Surface Integrity Implications

Progressive tool wear exerts deleterious effects on generated surface quality, with direct correlation established between flank wear magnitude and surface roughness degradation. As VB increases, the enlarged contact area between worn flank face and finished surface intensifies friction and plowing mechanisms, generating surface irregularities and residual stress concentrations. This wear-roughness coupling becomes particularly critical at elevated cutting speeds where accelerated wear progression compounds thermal effects, creating compounded deterioration of surface integrity.

The findings demonstrate that optimal cutting conditions must balance productivity considerations (maximized material removal rate) against tool life economics and surface quality requirements. For heat-treated XC18 steel machining with P35 inserts, recommended conditions of Vc = 120-150 m/min, f = 0.08-0.14 mm/rev, and ap = 0.5-0.75 mm provide favorable compromise, achieving acceptable surface finish while maintaining cutting temperatures below critical thermal degradation thresholds.

12. CONCLUSIONS

This comprehensive experimental investigation has provided fundamental insights into the complex thermomechanical phenomena governing the tool-workpiece-chip interface during hard turning operations. Through systematic thermal characterization and wear analysis across wide-ranging cutting parameters, the study elucidates critical interactions between process conditions, tool material properties, and workpiece metallurgical state that collectively determine machining performance and component quality.

The principal findings establish that cutting speed represents the dominant parameter influencing thermal generation, exhibiting exponential correlation with temperature rise across both P10 and P35 carbide insert grades. P35 tools demonstrate consistent thermal advantage, generating temperatures 15-40% lower than P10 counterparts depending on cutting conditions, attributed to superior wear resistance and optimized thermal properties. Heat treatment of XC18 steel workpieces yields measurable thermal benefits through microstructural refinement, facilitating more efficient chip formation with reduced energy dissipation.

Flank wear progression analysis confirms the superior longevity of P35 inserts, maintaining predictable linear wear accumulation over extended machining durations while P10 tools exhibit earlier onset of accelerated degradation. Critical thermal thresholds have been identified beyond which tool wear rates escalate dramatically, providing quantitative guidance for establishing safe operational boundaries.

The integration of thermal measurements with wear evolution data enables identification of optimal cutting parameter combinations that balance productivity requirements against tool life economics and surface integrity preservation. For heat-treated XC18 steel machining, recommended operating windows of Vc = 120-150 m/min, f = 0.08-0.14 mm/rev, and ap = 0.5-0.75 mm with P35 carbide inserts achieve favorable compromises, producing surfaces with beneficial residual stress distributions conducive to enhanced fatigue resistance while minimizing cutting forces and extending tool service life.

These findings contribute to the fundamental understanding of thermal management strategies in precision machining of hardened materials, providing experimentally validated guidelines for industrial implementation and establishing a foundation for development of predictive models enabling intelligent process optimization in advanced manufacturing environments.

13. REFERENCES

[1] M'Saoubi, R., Outeiro, J.C., Chandrasekaran, H., Dillon Jr, O.W., Jawahir, I.S., 2008. A review of surface integrity in machining and its impact on functional performance and life of machined products. International Journal of Sustainable Manufacturing 1(1-2), 203-236.
[2] Davim, J.P., 2011. Machining of Hard Materials. Springer-Verlag, London.
[3] Tönshoff, H.K., Arendt, C., Ben Amor, R., 2000. Cutting of hardened steel. CIRP Annals - Manufacturing Technology 49(2), 547-566.
[4] Grzesik, W., 2008. Advanced Machining Processes of Metallic Materials. Elsevier, Amsterdam.
[5] Bartarya, G., Choudhury, S.K., 2012. State of the art in hard turning. International Journal of Machine Tools and Manufacture 53(1), 1-14.
[6] Shaw, M.C., 2005. Metal Cutting Principles, 2nd ed. Oxford University Press, Oxford.
[7] Komanduri, R., Hou, Z.B., 2001. A review of the experimental techniques for the measurement of heat and temperatures generated in some manufacturing processes and tribology. Tribology International 34(10), 653-682.
[8] Lazoglu, I., Altintas, Y., 2002. Prediction of tool and chip temperature in continuous and interrupted machining. International Journal of Machine Tools and Manufacture 42(9), 1011-1022.

[9] Beno, J., Mankova, I., Vrabel, M., 2013. Experimental investigation of cutting temperature in high-speed machining. Advanced Materials Research 629, 81-86.
[10] Kitagawa, T., Kubo, A., Maekawa, K., 1997. Temperature and wear of cutting tools in high-speed machining of Inconel 718 and Ti-6Al-6V-2Sn. Wear 202(2), 142-148.
[11] Diniz, A.E., Oliveira, A.J., 2008. Optimizing the use of dry cutting in rough turning steel operations. International Journal of Machine Tools and Manufacture 48(9), 1009-1016.
[12] Sutter, G., Ranc, N., 2007. Temperature fields in a chip during high-speed orthogonal cutting—An experimental investigation. International Journal of Machine Tools and Manufacture 47(10), 1507-1517.
[13] Trigger, K.J., Chao, B.T., 1951. An analytical evaluation of metal cutting temperature. Transactions of the ASME 73, 57-68.
[14] Bacci da Silva, M., Wallbank, J., 1999. Cutting temperature: prediction and measurement methods—a review. Journal of Materials Processing Technology 88(1-3), 195-202.
[15] Ueda, T., Hosokawa, A., Oda, K., Yamada, K., 2001. Temperature on flank face of cutting tool in high speed milling. CIRP Annals - Manufacturing Technology 50(1), 37-40.
[16] O'Sullivan, D., Cotterell, M., 2001. Temperature measurement in single point turning. Journal of Materials Processing Technology 118(1-3), 301-308.
[17] Ay, H., Yang, W.J., 1998. Heat transfer and life of metal cutting tools in turning. International Journal of Heat and Mass Transfer 41(3), 613-623.
[18] Stephenson, D.A., 1993. Tool-work thermocouple temperature measurements—theory and implementation issues. Journal of Engineering for Industry 115(4), 432-437.
[19] Grzesik, W., Nieslony, P., 2004. Physics based modelling of interface temperatures in machining with multilayer coated tools at moderate cutting speeds. International Journal of Machine Tools and Manufacture 44(9), 889-901.
[20] Karpat, Y., Özel, T., 2008. Analytical and thermal modeling of high-speed machining with chamfered tools. Journal of Manufacturing Science and Engineering 130(1), 011001.
[21] Yvonnet, J., Umbrello, D., Chinesta, F., Micari, F., 2006. A simple inverse procedure to determine heat flux on the tool in orthogonal cutting. International Journal of Machine Tools and Manufacture 46(7-8), 820-827.
[22] Davim, J.P., Figueira, L., 2007. Machinability evaluation in hard turning of cold work tool steel (D2) with ceramic tools using statistical techniques. Materials & Design 28(4), 1186-1191.
[23] Abukhshim, N.A., Mativenga, P.T., Sheikh, M.A., 2006. Heat generation and temperature prediction in metal cutting: A review and implications for high speed machining. International Journal of Machine Tools and Manufacture 46(7-8), 782-800.
[24] Poulachon, G., Moisan, A.L., Jawahir, I.S., 2007. Tool-wear mechanisms in hard turning with polycrystalline cubic boron nitride tools. Wear 250(1-12), 576-586.
[25] Lima, J.G., Avila, R.F., Abrão, A.M., Faustino, M., Davim, J.P., 2005. Hard turning: AISI 4340 high strength low alloy steel and AISI D2 cold work tool steel. Journal of Materials Processing Technology 169(3), 388-395.
[26] Umbrello, D., M'Saoubi, R., Outeiro, J.C., 2007. The influence of Johnson–Cook material constants on finite element simulation of machining of AISI 316L steel. International Journal of Machine Tools and Manufacture 47(3-4), 462-470.
[27] Arrazola, P.J., Özel, T., Umbrello, D., Davies, M., Jawahir, I.S., 2013. Recent advances in modelling of metal machining processes. CIRP Annals - Manufacturing Technology 62(2), 695-718.
[28] Davies, M.A., Ueda, T., M'Saoubi, R., Mullany, B., Cooke, A.L., 2007. On the measurement of temperature in material removal processes. CIRP Annals - Manufacturing Technology 56(2), 581-604.
[29] Le Coz, G., Marinescu, M., Devillez, A., Dudzinski, D., Velnom, L., 2012. Measuring temperature of rotating cutting tools: Application to MQL drilling and dry milling of aerospace alloys. Applied Thermal Engineering 36, 434-441.

[30] Ueda, T., Sato, M., Nakayama, K., 1998. The temperature of a single crystal diamond tool in turning. CIRP Annals - Manufacturing Technology 47(1), 41-44.
[31] Ay, H., Yang, W.J., 1998. Heat transfer and life of metal cutting tools in turning. International Journal of Heat and Mass Transfer 41(3), 613-623.
[32] Kwon, P., Schiemann, T., Kountanya, R., 2001. An inverse estimation scheme to measure steady-state tool-chip interface temperatures using an infrared camera. International Journal of Machine Tools and Manufacture 41(7), 1015-1030.
[33] Kitagawa, T., Kubo, A., Maekawa, K., 1997. Temperature and wear of cutting tools in high-speed machining of Inconel 718 and Ti-6Al-6V-2Sn. Wear 202(2), 142-148.
[34] Trigger, K.J., Chao, B.T., 1951. An analytical evaluation of metal cutting temperature. Transactions of the ASME 73, 57-68.
[35] Stephenson, D.A., 1993. Tool-work thermocouple temperature measurements—theory and implementation issues. Journal of Engineering for Industry 115(4), 432-437.
[36] Kus, A., Isik, Y., Cakir, M.C., Coşkun, S., Özdemir, K., 2015. Thermocouple and infrared sensor-based measurement of temperature distribution in metal cutting. Sensors 15(1), 1274-1291.
[37] O'Sullivan, D., Cotterell, M., 2001. Temperature measurement in single point turning. Journal of Materials Processing Technology 118(1-3), 301-308.
[38] Sutter, G., Ranc, N., 2007. Temperature fields in a chip during high-speed orthogonal cutting—An experimental investigation. International Journal of Machine Tools and Manufacture 47(10), 1507-1517.
[39] Müller, B., Renz, U., 2003. Time resolved temperature measurements in manufacturing. Measurement 34(4), 363-370.
[40] Ueda, T., Hosokawa, A., Oda, K., Yamada, K., 2001. Temperature on flank face of cutting tool in high speed milling. CIRP Annals - Manufacturing Technology 50(1), 37-40.
[41] Sutter, G., Faure, L., Molinari, A., Ranc, N., Pina, V., 2003. An experimental technique for the measurement of temperature fields for the orthogonal cutting in high speed machining. International Journal of Machine Tools and Manufacture 43(7), 671-678.
[42] Arrazola, P.J., Arriola, I., Davies, M.A., Cooke, A.L., Dutterer, B.S., 2008. The effect of machinability on thermal fields in orthogonal cutting of AISI 4140 steel. CIRP Annals - Manufacturing Technology 57(1), 65-68.
[43] Outeiro, J.C., Umbrello, D., M'Saoubi, R., 2006. Experimental and numerical modelling of the residual stresses induced in orthogonal cutting of AISI 316L steel. International Journal of Machine Tools and Manufacture 46(14), 1786-1794.
[44] Grzesik, W., Żak, K., 2012. Modification of surface finish produced by hard turning using superfinishing and burnishing operations. Journal of Materials Processing Technology 212(1), 315-322.
[45] Griffiths, B.J., 1987. Mechanisms of white layer generation with reference to machining and deformation processes. Journal of Tribology 109(3), 525-530.
[46] Amri. B, Contribution à l'étude du comportement des matériaux modernes pour outils coupants, Thèse, INSA-Lyon, pp43-44, 1987.
[47] Bacci. M, J, Wallbank J, Cutting temperature prediction and measurement methods-a review, J. Mater. Process. Technol. N°88, pp195-202, 1999.
[48] Smart, E.F., Trent, E.M., 1975. Temperature distribution in tools used for cutting iron, titanium and nickel. International Journal of Production Research 13(3), 265-290.
[49] Boothroyd, G., 1963. Temperatures in orthogonal metal cutting. Proceedings of the Institution of Mechanical Engineers 177(1), 789-810.
[50] Childs, T.H.C., 2013. Metal Machining: Theory and Applications. Butterworth-Heinemann, Oxford.
[51] Abukhshim, N.A., Mativenga, P.T., Sheikh, M.A., 2006. Heat generation and temperature prediction in metal cutting: A review and implications for high speed machining. International Journal of Machine Tools and Manufacture 46(7-8), 782-800.

[52] Diniz, A.E., Oliveira, A.J., 2008. Optimizing the use of dry cutting in rough turning steel operations. International Journal of Machine Tools and Manufacture 48(9), 1009-1016.
[53] Komanduri, R., Hou, Z.B., 2001. A review of the experimental techniques for the measurement of heat and temperatures generated in some manufacturing processes and tribology. Tribology International 34(10), 653-682.
[54] Bacci da Silva, M., Wallbank, J., 1999. Cutting temperature: prediction and measurement methods—a review. Journal of Materials Processing Technology 88(1-3), 195-202.
[55] Lazoglu, I., Altintas, Y., 2002. Prediction of tool and chip temperature in continuous and interrupted machining. International Journal of Machine Tools and Manufacture 42(9), 1011-1022.
[56] Grzesik, W., Nieslony, P., 2004. Physics based modelling of interface temperatures in machining with multilayer coated tools at moderate cutting speeds. International Journal of Machine Tools and Manufacture 44(9), 889-901.
[57] ASM International, 1990. ASM Handbook Volume 1: Properties and Selection: Irons, Steels, and High-Performance Alloys. ASM International, Materials Park, OH.
[58] Rech, J., Moisan, A., 2003. Surface integrity in finish hard turning of case-hardened steels. International Journal of Machine Tools and Manufacture 43(5), 543-550.
[59] Astakhov, V.P., 2006. Tribology of Metal Cutting. Elsevier, London.
[60] Özel, T., Karpat, Y., 2005. Predictive modeling of surface roughness and tool wear in hard turning using regression and neural networks. International Journal of Machine Tools and Manufacture 45(4-5), 467-479.
[61] Chou, Y.K., Evans, C.J., 1999. White layers and thermal modeling of hard turned surfaces. International Journal of Machine Tools and Manufacture 39(12), 1863-1881.
[62] Bourdim, M., 2013. Contribution à l'étude de l'intégrité de l'état de surface usinée en tournage dur. Thèse de doctorat, ENSET Oran.
[60] Totten, G.E., Howes, M.A.H., 1997. Steel Heat Treatment Handbook. Marcel Dekker, New York.

[62] Andonov, I., Bekech, Y., 1984. Analyse et synthèse des processus technologiques en construction mécanique. Technica, Sofia.
[63] Barlier, C., Girardin, L., 1992. Mémotechmatériaux et usinage. Editions Casteilla, pp. 137-140.
[64] Peigne, G., 2003. Etude et simulation des effets dynamiques de la coupe sur la stabilité de la coupe et la qualité géométrique de la surface usinée, application au fraisage de profil. Thèse de doctorat, Institut Polytechnique de Grenoble.
[65] Kurita, T., Chikamori, K., Kubota, S., Hattori, M., 2006. A study of three-dimensional shape machining with an ECμM system. International Journal of Machine Tools and Manufacture 46(12-13), 1311-1318.
[66] Choi, S., et al., 2007. Fabrication of WC microshaft by using electrochemical etching. The International Journal of Advanced Manufacturing Technology 31(7), 682-687.
[67] Brinksmeier, E., Preuss, W., 2012. Micromachining ultra-precision engineering from physics to manufacturing. Royal Society.